

Physicochemical interactions in antimicrobial cotton fabrics functionalized with CuO_x grown *in situ*

Luz E. Román[§], Carmen Uribe[¶], Francisco Paraguay-Delgado[‡], James G. Sutjianto[◊], Enrique D. Gómez^{◊,▲}, José L. Solís[§], Mónica M. Gómez^{§}*

[§]Faculty of Science, Universidad Nacional de Ingeniería, Av. Túpac Amaru 210, Lima 15333, Peru

[¶]Facultad de Ingeniería Química y Textil, Universidad Nacional de Ingeniería, Av. Túpac Amaru 210, Lima 15333, Peru

[‡]Centro de Investigación en Materiales Avanzados, S.C. (CIMAV), Av. Miguel de Cervantes #120, Complejo Industrial Chihuahua, Chihuahua, Chih CP 31136, México;

[◊]Department of Chemical Engineering, The Pennsylvania State University, University Park, PA 16802, USA;

^{*}Department of Materials Science and Engineering, Materials Research Institute, The Pennsylvania State University, University Park, PA 16802, USA

KEYWORDS: Cotton, cellulose, copper oxides, copper salts, cuprous oxide, cupric oxide, antimicrobial

ABSTRACT

The appearance and spread of harmful microorganisms represent challenges to public and private health. Antimicrobial cotton textiles functionalized with semiconductor oxides offer a potential solution to reduce the spread of various pathogens. Here, we study the physicochemical interactions between copper oxides (CuO_x) and cellulose in cotton fiber functionalized with these same oxides for antimicrobial properties. Fabrics were treated via an exhaust dyeing method using 2% on-weight-of-fiber (owf) copper precursor with acetate, nitrate, and sulfate anions and 0.5 g/L of NaOH. Non-functionalized (NF) fabric and fabrics functionalized with CuO_x were evaluated by colorimetry within CIELab and characterized by inductively coupled plasma mass spectrometry (ICP-MS), X-ray photoelectron spectroscopy (XPS), transmission electron microscope (TEM), electron diffraction patterns (SAED), secondary ions in time-of-flight (TOF-SIMS), and scanning electron microscopy (SEM). Additionally, antimicrobial activity was measured against *Escherichia coli* and *Pseudomonas aeruginosa* strains according to the ASTM E2149 standard. The non-functionalized (NF) fabrics with a yellow hue turned reddish brown after the functionalization process due to the presence of CuO_x . The amount of copper (Cu) in the functionalized fabrics with copper oxides increased to 27 to 40% of the bath Cu concentration compared to 0.009% in the NF fabric. XPS analysis for cotton suggest a chemical interaction between the hydroxyl groups of cellulose and CuO_x . Furthermore, the spectra of functionalized fabrics exhibited peaks corresponding to Cu^{1+} and Cu^{2+} ions, assigned to the Cu_2O and CuO phases, respectively. Electron diffraction patterns confirmed copper oxide crystalline phases, where Cu_2O was indexed in the cuprite system and CuO in tenorite system. Likewise, all fabrics functionalized with CuO_x inhibited the growth of the two strains analyzed by more than 99%.

Therefore, cotton fabrics functionalized with the mixture of Cu₂O and CuO have excellent antimicrobial properties that can be used in environments with a high bacterial load.

1. INTRODUCTION

The development and application of antimicrobial textiles are growing in interest and importance. The COVID-19 pandemic has increased awareness of the importance of limiting pathogen spread, and has generated greater consumption of certain products and textile materials with antimicrobial properties.^{1, 2} Antimicrobial fabrics can inhibit the growth and propagation of microorganisms, such as bacteria, viruses, and fungi.³ A common approach to achieving antimicrobial properties in textiles is through *in-situ* or *ex-situ* incorporation of metal oxides into fibers or as surface coatings.⁴ These metal oxides, such as copper, zinc, titanium, and silver, have been shown to reduce microbial growth.⁵⁻⁸

The versatility and cost-effectiveness of copper allows applications in a variety of fields, such as electrochemistry,⁹ catalysis,¹⁰ energy production and storage,¹¹ and pharmaceuticals.¹² Copper oxides (CuO_x), such as cuprous oxide (Cu₂O) and cupric oxide (CuO), are stable and long-lived. They are used in commercial products, such as agrochemicals, paints, cosmetics, medical devices, and antimicrobial agents.¹³ The latter use arises from efficient antiviral, antifungal, and antibacterial characteristics of copper oxides.¹⁴ Thus, functionalization of materials, such as textiles, has emerged as a promising approach for imparting antimicrobial properties for end-user applications.^{15, 16}

Some textiles functionalized with CuO_x retain their antimicrobial properties even after multiple wash cycles, while others do not. El-Nahhal *et al.* have developed cotton fibers with antimicrobial properties using ultrasonic irradiation.¹⁷ The cotton fabric was pre-treated with starch using three

concentrations (1, 2, and 3 starch wt. %). The cotton fabric and starched cotton fabric were *in situ* coated in the presence of sodium hydroxide with CuO nanoparticles (NPs) synthesized from copper acetate. After ten domestic washes, the antibacterial reduction of cotton fabric functionalized with CuO NPs was 48% for *Escherichia coli* (*E. coli*) and 69% for *Staphylococcus aureus* (*S. aureus*), in contrast to the cotton fiber with 3% starch content and coated with CuO NPs, whose antibacterial activity remained above 92% against the same bacteria.

Hillyer *et al.* synthesized *in situ* Cu₂O nanoflowers on cotton fibers, and they demonstrated that, even after 50 laundering cycles, the antimicrobial activity of functionalized cotton fabrics persisted with greater than 99% inhibition against *Klebsiella pneumonia* (*K. pneumonia*), *E. coli*, *S. aureus* and *Aspergillus niger* (*A. niger*), and more than 90% inhibition against Human coronavirus (strain 229E).¹³ The authors proposed that Cu²⁺ ions were incorporated within the β (1–4) linked D-glucose chain of cellulose and, after neutralization, were reduced and formed Cu₂O on the fabric.

The report by Zarbaf *et al.* showed the *in situ* synthesis of CuO_x NPs in a 100% cotton denim fabric to impart antibacterial properties.¹⁸ Samples were treated with a mixture of copper sulfate, sodium hydroxide, and glucose. X-ray diffraction determined the presence of Cu₂O and CuO in the samples, with and without glucose content. The denim samples inhibit the growth of *E. coli* and *S. aureus* bacteria, even after 30 wash cycles. The authors also proposed a series of reactions between the reagents and cellulose. Copper sulfate and sodium hydroxide leads to copper hydroxide (Cu(OH)₂), which in contact with cotton cellulose produces a mixture of CuO and Cu₂O nanoparticles on the surface of denim.

Here, we expand on the aforementioned work to identify key physicochemical interactions between cotton cellulose and copper oxides, and how these depend on precursor chemistry. CuO_x

was synthesized from copper acetate, nitrate and sulfate salts, and a reducing agent on the surface of cotton textiles. The *in situ* functionalization of cotton fabrics with CuO_x was performed by a conventional dyeing method, exhaust dyeing, which employs high-temperature dyeing equipment (HTDE) commonly used for wet processing throughout the textile industry. Cotton fabrics functionalized with CuO_x using different copper salts were analyzed using the CIELab colorimetric method. Elemental concentrations of copper on the fabrics before and after functionalization were determined using ICP-MS. In addition, surface characterization was carried out using XPS and TOF-SIMS, and particle structure and morphology were characterized using SEM and SAED. The antimicrobial activity of the fabrics was evaluated using American Society for Testing and Materials (ASTM) E2149 standard against *E. coli* and *Pseudomonas aeruginosa* (*P. aeruginosa*).

2. EXPERIMENTAL SECTION

2.1. Materials

All chemicals used were analytical grade. Copper acetate monohydrate (99% pure) and copper nitrate trihydrate (99% pure) were supplied by Merck. Copper sulfate pentahydrate (99% pure) was provided by the local store, J.A. Elmer. Sodium hydroxide (98.5% pure) was purchased from Sharlau. Twill weave 100% cotton fabric with 296.41 g/m² was supplied by the local factory Tejidos San Jacinto S.A. which was previously subjected to a scouring and bleaching process, making cotton material ready-to-dye. All solutions were made using distilled water. Other chemicals and equipment employed in this study are described in the following subsections.

2.2. Functionalization process

The functionalization process is similar to the procedure presented by Villalva.¹⁹ Figure 1 shows the functionalization curve and the fabrics sampling along the curve. The *in situ* synthesis of the CuO_x on the cotton fabric was carried out via an exhaust dyeing method using Rapid Eco Dyer-24 HTDE equipment. The copper acetate monohydrate (Cu(CH₃COO)₂ · H₂O), copper nitrate trihydrate (Cu(NO₃)₂ · 3H₂O), and copper sulfate pentahydrate (CuSO₄ · 5H₂O) concentrations used were 2% on-weight-fabric (owf), and that of sodium hydroxide (NaOH) was 0.5 g/L. An exhaustion bath at a liquor ratio of 10:1 (LR) was prepared from copper salts. Liquor ratio could be defined as the volume of liquor to be taken in dyebath in proportion to the weight of the textile and is denoted by LR.²⁰ Five grams of ready-to-dye cotton fabric were immersed in a 50-mL exhaustion bath in a steel beaker; the beaker was then closed and introduced in the HTDE. The solution remained under constant stirring at 50 rpm for 90 min at room temperature; this stage is known as primary exhaustion at an acidic pH of 5. After this time, the copper salt solutions were discarded. Subsequently, 50 mL of the distilled water was added to the steel beaker. The steel beaker was again placed inside the HTDE and stirred for 10 min at 60 °C. Then, a first dosage was made by adding 83 µL of a stock solution to the beaker. Stock solution was prepared by dissolving 1 g of NaOH in 10 mL of distilled water. Ten minutes later, a second dosing was done with 167 µL of the same stock solution. Once the dosages were finished, the steel beaker was stirred for another 10 min. Afterward, the temperature of the HTDE was increased to 90 °C and kept under constant stirring for 20 min. This process stage is called secondary exhaustion at a basic pH of 11. Then, the cotton fabric was rinsed with hot water at 70 °C and cold at room temperature, neutralized with 0.5 g/L acetic acid solution, rinsed again with distilled water, and dried at 80 °C in a Rapid CO laboratory mini-dryer. This stage is known as subsequent processes.

Samples were taken from different sites within the functionalization curve with the following characteristics: (1) fabric at 25 °C with copper salt obtained at the end of the primary exhaustion stage; (2) fabric at 60 °C with copper salt and after adding NaOH; (3) fabric at 90 °C with copper salt and NaOH; (4) fabric at 70 °C functionalized with CuO_x; and (5) fabric functionalized after subsequent processes stage.

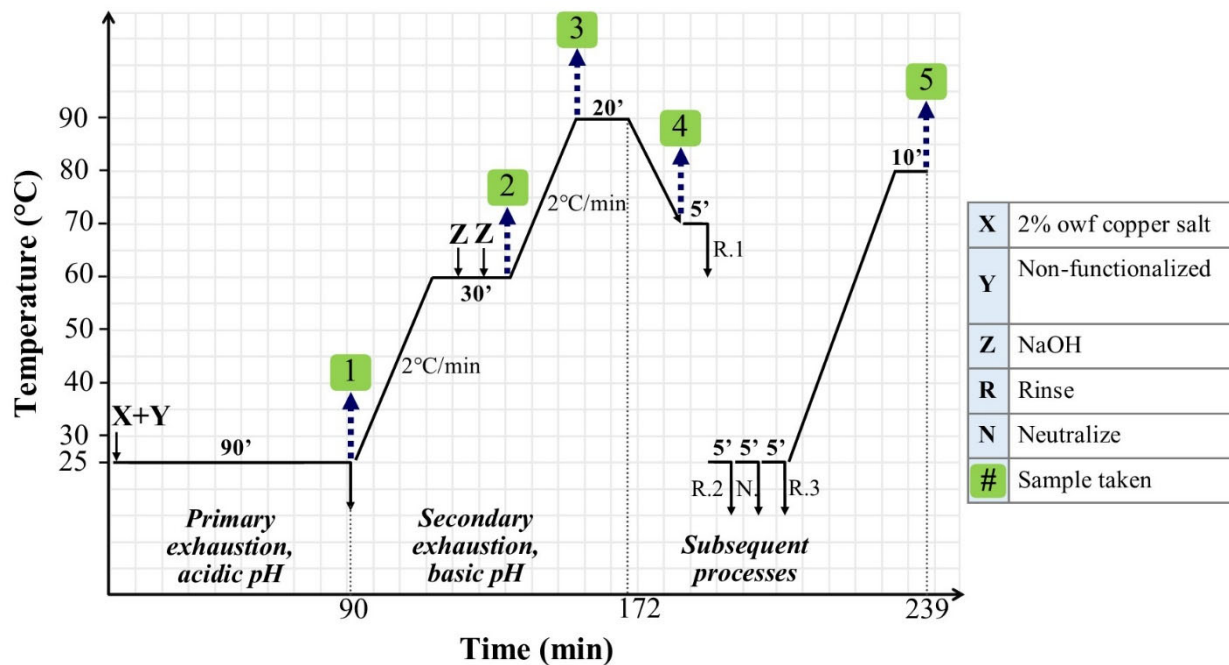


Figure 1. Functionalization sequence of cotton fabric with copper oxides and fabrics sampling sites.

2.3. Physical characterization

2.3.1. Colorimetric characteristics

The colorimetric characteristics of the cotton fabrics were evaluated using a Datacolor 550 visible spectrophotometer (Datacolor) calibrated with specular included, small area view, and UV filter included (OFF). Thirty-one reflectance spectral values were obtained in the visible spectrum range from 400 to 700 nm, which were transformed into CIE L*a*b* color coordinates for a D65 light source with a viewing angle of 10° using Datacolor TOOLS version 1.1 software, where L* is lightness, a* is red-green value, and b* is blue– yellow value.

2.3.2. Inductively coupled plasma mass spectrometry (ICP-MS)

The amount of copper present in the exhaustion baths prepared from the three copper salts in the non-functionalized fabric and the samples taken during the functionalization process with CuO_x was obtained on an iCAP RQplus inductively coupled plasma mass spectrometer (Thermo Fisher Scientific). The fabric samples were prepared using the digestion method of nitric acid.

2.3.3. X-ray photoelectron spectroscopy (XPS)

X-ray photoelectron spectra of non-functionalized fabric and samples taken during the functionalization process with CuO_x were acquired using an Escalab 250 Xi X-ray photoelectron spectrometer (Thermo Fisher Scientific). The excitation source was monochromatic Al K α radiation ($h\nu = 1486.6$ eV), and the analyzer pass energy was set to 20 eV with an energy step size of 0.1 eV.

2.3.4. Time-of-flight secondary ion mass spectrometry (TOF-SIMS)

Time-of-flight secondary ion mass spectrometry was obtained positive ion mass spectra of non-functionalized fabric and functionalized fabrics with CuO_x. These analyses were conducted using a TOF.SIMS 5 instrument (ION TOF) equipped with bismuth liquid metal ion gun (Bi_n^{m+}; n = 1 -

5, m = 1, 2). For high mass resolution spectra acquired in this research, a pulsed Bi³⁺ primary ion beam with an incident angle of 45° impact energy of 25 keV was used. The positive secondary ion mass spectra were calibrated using H⁺, C⁺, C₂H₃⁺, C₃H₅⁺, and C₄H₇⁺.

2.3.5. *Selected area electron diffraction (SAED) pattern*

The particles were obtained by untangling the fabric's cotton fibers functionalized with CuO_x from three copper salts. These untangled fibers were introduced into a vial containing isopropyl alcohol and sonicated for 10 min. Then, two drops of the obtained supernatant were placed onto a lacey carbon film with a continuous carbon film layer on a nickel grid with 400-mesh for characterization. Transmission electron microscope (TEM) images and electron diffraction patterns (SAED) from the particles were acquired with a JEOL JEM2200FS microscope operated at 200 kV. The images and electron diffraction patterns were acquired from different zones and indexed by measuring the distances between two symmetrical spot patterns using Digital Micrograph® software.

2.3.6. *Scanning electron microscopy (SEM)*

The morphology characterization of the fabrics was visualized with an Apreo 5 scanning electron microscope (Thermo Fisher Scientific). Before SEM imaging, the cotton fabrics were coated with a thin 6 nm thick iridium layer. The images were obtained at 5,000 to 120,000 times magnification.

2.4. Antibacterial evaluation

A quantitative method was applied to evaluate the antimicrobial activity of the functionalized cotton fabrics based on the ASTM E2149 protocol. *E. coli* ATCC 25922 and *P. aeruginosa* ATCC 10145 were cultured for 18 h at 35 °C in sterile tryptic soy broth (TSB). At the end of this time,

the TSB with the strains was centrifuged at 4000 rpm for 5 min. The cultures obtained were washed twice with a sterile buffer solution (0.3 mM KH₂PO₄). Afterward, the culture was diluted with the sterile buffer until obtaining a final concentration of 1.5-3.0x10⁵ colony-forming units per milliliter (CFU/mL). This solution was the working bacterial dilution. The non-functionalized and functionalized fabrics with CuO_x were sterilized by autoclaving at 121 °C for 15 min. One gram of sterile fabrics was placed inside an Erlenmeyer flask containing 50 mL of the working bacterial dilution. The flasks were incubated at 35 °C and continuously shaken at a maximum stroke for 1 h. After incubation, the buffer solution in the flask was serially diluted, and fractions were plated on a Petri dish with tryptic soy agar (TSA). All the Petri dishes were incubated at 35 °C for 24 h. Subsequently, the count of colonies was performed. The CFU/mL was calculated by multiplying the number of colonies by the dilution factor. The results of the antimicrobial evaluation were expressed as a percentage reduction of organisms, and it was calculated using the following equation 1.

$$\text{Reduction, \% (CFU/mL)} = \frac{C - A}{C} \times 100\% \quad (1)$$

In this equation, A is the CFU/mL value for the flask containing the functionalized fabric, and C is the CFU/mL for the flask containing the non-functionalized fabric after 1h contact time.

3. RESULTS AND DISCUSSION

3.1. Cotton fabric functionalized with CuO_x and colorimetry

Functionalization of twill cotton fabrics with CuO_x was carried out using 2% owf of each Cu(CH₃COO)₂ H₂O, Cu(NO₃)₂ 3H₂O, and CuSO₄ 5H₂O with 0.5 g/L NaOH for each case. Table

1 presents the nomenclature of the fabric samples, and it includes the type of copper salt (A = acetate, N = Nitrate, S = Sulfate), followed by a number indicating the sampling sites on the functionalization curve (Figure 1), as detailed in section 2.2.

Table 1. Nomenclature of fabric samples obtained before, during, and after the functionalization process with CuO_x.

Process stage of cotton fabrics	Salts sources		
	Copper acetate	Copper nitrate	Copper sulfate
Non-functionalized	NF		
At 25°C with copper salt	A1	N1	S1
At 60°C with copper salt + NaOH	A2	N2	S2
At 90°C with copper salt + NaOH	A3	N3	S3
At 70°C functionalized with CuO _x	A4	N4	S4
Fabric functionalized after subsequent processes stage	A5	N5	S5

Photographs of non-functionalized fabric and of the fabric samples taken from different sites during the functionalization curve with CuO_x using 2% owf of Cu(CH₃COO)₂ H₂O, Cu(NO₃)₂ 3H₂O and CuSO₄ 5H₂O; and 0.5 g/L of NaOH, are shown in Figure 2(a), (b) and (c), respectively. The hue of the NF fabrics changes at the different stages of the functionalization process for the three copper salt sources. We further discuss a detailed colorimetric description of each sample below.

Figures 2(d) and 2(e) provide the color space coordinates in the CIE L*a*b* colorimetric system of non-functionalized fabric and fabrics taken during the functionalization process with CuO_x. The NF fabric has a lightness value (L*) of 93.61 and a* and b* values of -0.55 and 5.01, respectively. These values indicate that the sample has a yellow hue with high luminosity. After the primary exhausting stage, L* decreases slightly to values of 89.12, 90.27, and 90.28 for A1, N1, and S1, respectively. Likewise, b* decreases, reaching values of 2.82 for A1, 3.19 for N1, and 3.23 for S1. In the case of the a* coordinate, a substantial decrease is apparent, and minimum values reach -6.28, -4.88, and -4.84 for A1, N1, and S1, respectively. Thus, the changes in CIE L*a*b* coordinates, especially in a*, indicate the acquisition of a yellow-greenish hue, as seen in the photographs of the A1, N1, and S1 samples (Figure 2(a-c)). According to Cotton *et al.*, Cu (II) salts dissolved in water form a hexaaquacopper (II) complex ion [Cu(H₂O)₆]²⁺ that has a blue or green color;²¹ therefore, the yellow-greenish hue may be associated with the presence of copper (II) complexes in fabrics.

After NaOH addition at 60°C, the luminosity of A2, N2, and S2 samples continued to decrease to 86.51, 86.54, and 86.97, respectively. Their a* and b* color coordinates show slight variations between 0.25 and 0.57. The fabrics become slightly darker after NaOH treatment, but do not change their greenish hue.

Upon reaching the predetermined temperature of 90 °C, copper oxides begin to form, and their initial presence in fabrics was evidenced by a substantial reduction in luminosity and a rise towards a red hue; that is, there is an increase in a* towards positive values. The a* values of A3 and N3 increase as +0.91 and +0.09, respectively, and L* values are 76.7 for A3 and 80.1 for N3. These changes indicate a variation in hue of the fabrics towards dark brown. In the S3 sample, the a* coordinate increases 2.37 points but remains negative, with a final value of -2.52. Therefore, its

hue was less green and slightly darker. The dark hue of A3, N3, and S3 samples can be seen in Figure 2(a-c). After 20 min of stirring at 90 °C and cooling to 70 °C, the A4, N4, and S4 samples decreased in luminosity and reach minimum values of 74.89, 77.48, and 77.02, respectively. Meanwhile, a^* of the same samples presents maximum values of 1.78, 1.41, and 1.33 for A4, N4 and S4, respectively. These outcomes imply that these fabrics presented a reddish-brown hue that is darker than the aforementioned samples (A3, N3, and S3).

Huang *et al.* reported that the hue of polyester fiber fabrics coated with copper oxides changed from brown to dark red as the luminosity decreased; they also mentioned that the content of Cu^{1+} and Cu^{2+} ions influenced the hue of the textile.²² Thus, the increase in reddish hue and low luminosity of A4, N4, and S4 samples can be a result of CuO_x synthesized *in situ* on cotton fabrics. After rinsing and neutralization, the luminosity of A5, N5, and S5 samples increases by around 5% when compared to A4, N4, and S4. This increase is likely from removal of physically adsorbed copper oxides from the surface of cotton fibers, resulting in lighter fabrics with a less red-brown hue. Therefore, non-functionalized fabrics with a yellow hue and high luminosity turned greenish and finally reddish brown during the functionalization with 2% owf of copper salt, likely from the presence of copper oxides.

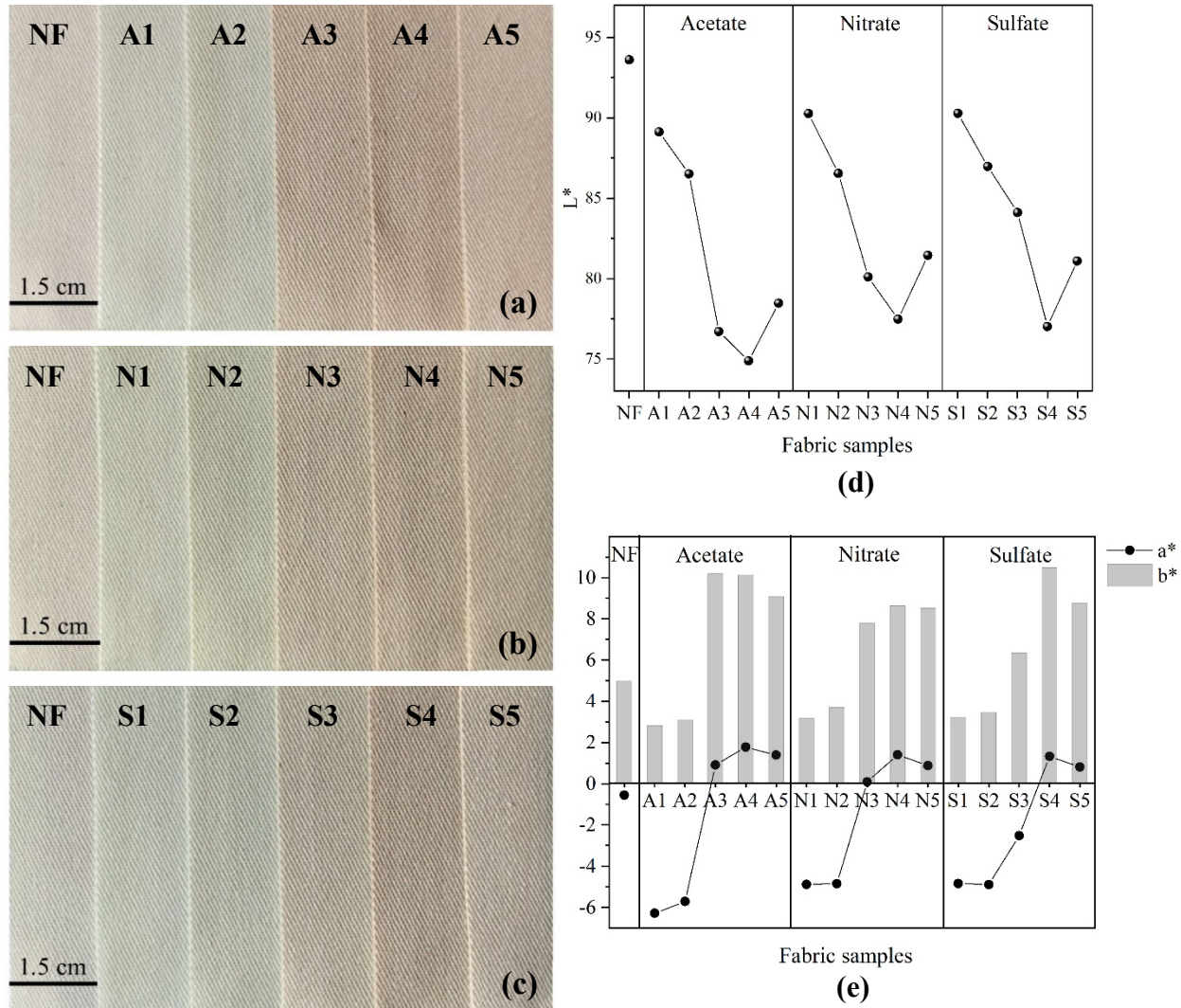


Figure 2. Photographs of non-functionalized fabric and fabrics taken during the functionalization process with CuO_x from copper salts of (a) acetate, (b) nitrate, and (c) sulfate, and CIE $L^*a^*b^*$ color coordinates of these same fabrics: (d) Luminosity - L^* ; and (e) a^* and b^* values.

3.2. Fabric characterizations

Elemental chemical analysis was carried out using ICP-MS to determine the copper (Cu) concentration in the liquid and solid samples. Figure 3 presents the Cu amount in exhaustion baths prepared from the three copper salts in non-functionalized fabric and the fabrics taken during the functionalization process. The amounts of Cu in the exhaustion baths prepared from copper acetate, nitrate, and sulfate salts were 4956, 5410, and 5221 mg/L, respectively. We take these values as the initial copper amount, representing a 100% concentration. In the exhaustion dyeing process, dye molecules dissolve in the bath, are adsorbed by the textile, and diffuse into fibers, thus resulting in a decrease in dye concentration of the bath and an increase in dye concentration in the textile.^{23, 24} Indeed, after the primary exhaustion at an acidic pH, the initial Cu concentration increases from 0.009% in the NF sample to 54, 42, and 42% of the Cu amount in the baths for A1, N1, and S1, respectively. Thus, copper from the exhaustion baths was adsorbed onto cotton fibers.

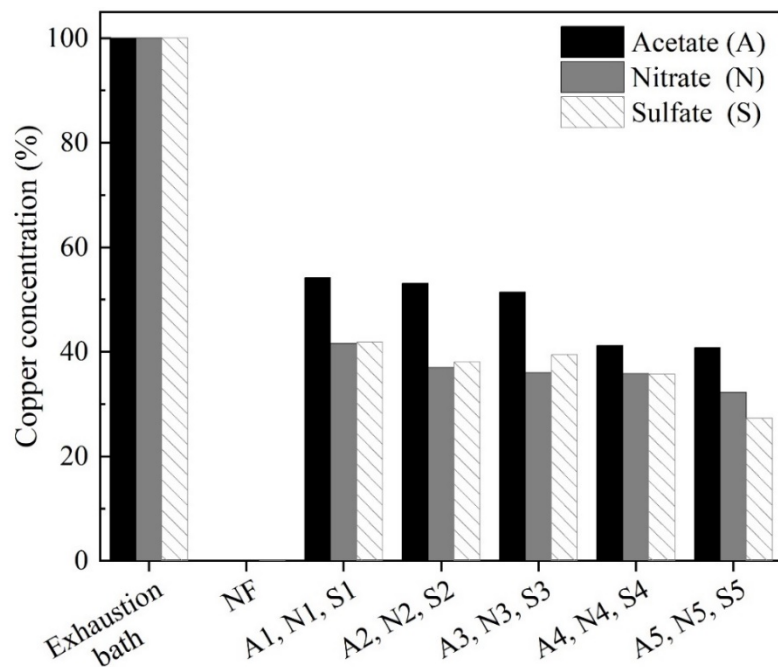


Figure 3. Amount of Cu determined by ICP-MS in exhaustion baths, non-functionalized fabric, and in fabrics taken during the functionalization process with CuO_x from copper acetate, nitrate, and sulfate.

These results show that cotton absorbs more Cu when a copper acetate salt is used. This could be a result of the chemical affinity between acetate ions and cotton cellulose. Mature cotton fibers contains around 88 to 99 wt% cellulose, with a molecular structure composed of C, O, and H atoms.^{25,26} The acetate ion (CH₃COO⁻) may have a more substantial attraction to cellulose, perhaps due to stronger hydrogen bonding, when compared to nitrate (NO₃⁻) and sulfate (SO₄²⁻) ions. For A1, N1, and S1 samples, after adding NaOH the amount of Cu decreases by about 1, 5, and 4% for A2, N2, and S2, respectively. Increasing the temperature to 90 °C leads to another drop in Cu of 3% for A3, 6% for N3, and 2% for S3. These decrease are likely from Cu release from the cotton fabric towards the volume of water added at the beginning of the secondary exhaustion, such that Cu particles could be present in the liquid phase.

After 20 min of stirring at 90 °C and cooling to 70 °C, the Cu amount in A4, N4, and S4 continues to decrease, by 13, 6, and 6%, respectively. This decrease can be attributed to the continuous release of Cu from cotton into the aqueous medium. In subsequent processes, the Cu amount continues to decrease, likely from loss of CuO_x that is not bound to cotton fibers.²⁷ The final Cu concentration in the fabrics is approximately 40% for A5, 32% for N5, and 27% for S5. Thus, over 60% of the Cu in the exhaustion baths is lost in wastewater from primary and secondary exhaustion baths and subsequent processes. The limited conversion into bound CuO_x is not unexpected, as

others have shown²⁸ that functionalization of textiles prior to treatment with metal oxides is often needed to maximize uptake and long-term fixation.

We confirm CuO_x functionalization through surface analyses. Figure 4(a-c) shows the broad XPS spectrum of the NF sample, which shows oxygen peaks such as O1, O2, OKL1, OKL2, and carbon peaks such as C1 and CKL1; these peaks are attributed to cotton fibers.^{15,29} Samples after treatment with copper salts show Cu 2p peaks, including from A1, A4, A5, N1, N4, N5, S1, S4 and S5. XPS confirms the presence of Cu in our samples, and detailed analysis of the spectra can reveal changes in bonding states of constituent elements.

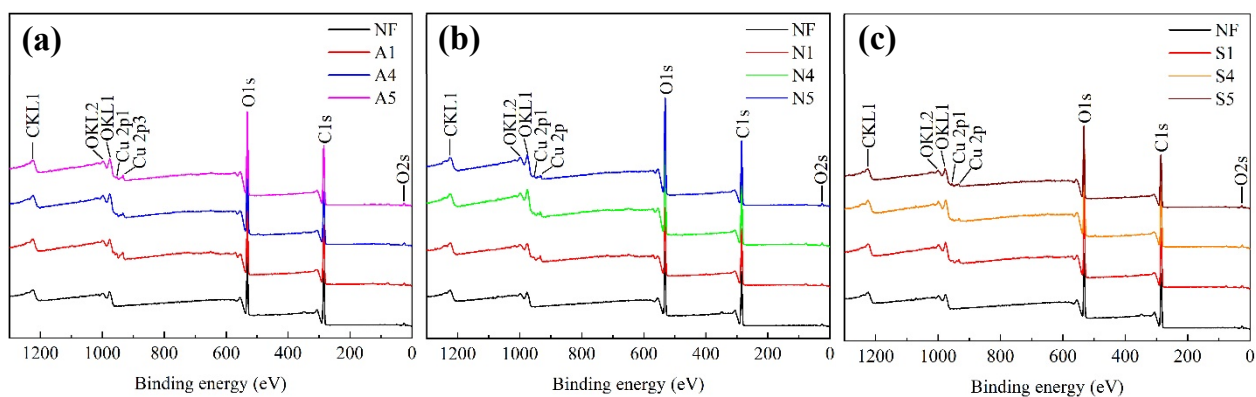


Figure 4. Broad XPS spectrum of non-functionalized fabric and fabrics taken during the functionalization process with CuO_x from (a) acetate, (b) nitrate, and (c) sulfate copper salts sources, respectively.

The high-resolution C 1s spectra of the NF sample and samples obtained after CuO_x treatment are shown in Figure 5(a). The carbon (C 1s) spectrum for cotton can be deconvoluted into three contributions: C1, C2, and C3. The C1 corresponds to carbon atoms bonded only with carbon or hydrogen atoms (-C-C, -C-H); C2 belongs to carbon atoms bonded with a single bond to an oxygen

atom (-C-O), and; C3 represents carbon atoms bonded to one oxygen atom by double bond or by a single bond to two oxygen atoms (-C=O or O-C-O).^{29,30}

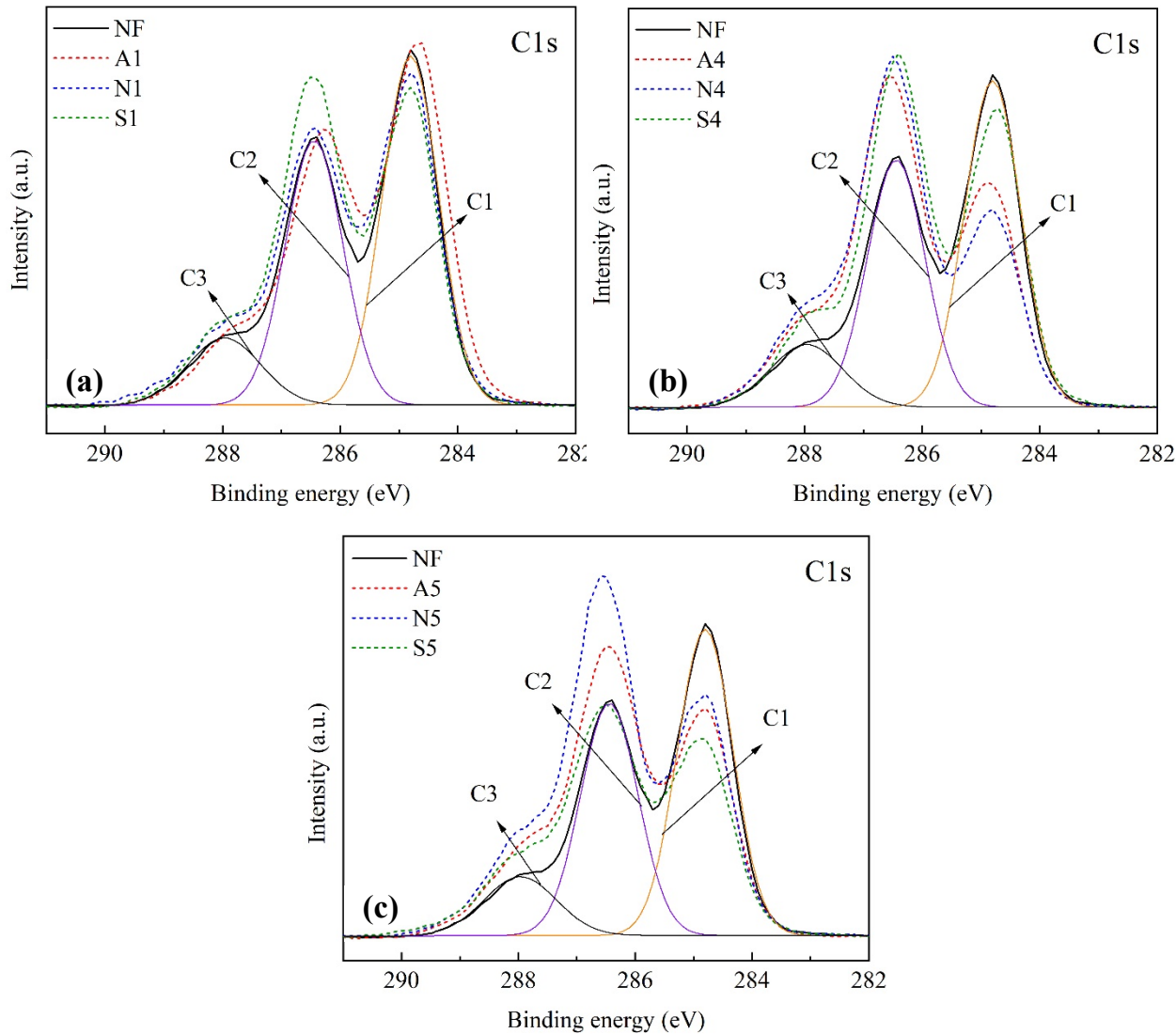


Figure 5. XPS spectra of C 1s in non-functionalized fabric and fabrics taken: (a) at 25 °C with copper salts (primary exhaustion stage), (b) after the addition of NaOH, temperature increase to 90 °C and cooling to 70 °C (secondary exhaustion stage), and (c) functionalized with CuO_x after rinses and neutralization (subsequent processes stage).

After the first stage, there is a reduction in the spectral contribution of the C1 component, of approximately 1, 2 and 9% for A1, N1 and S1, respectively, when compared to NF (Figure 5a). In the case of C2, the spectral contribution of N1 experienced a reduction of 1%, while in A1 and S1 the contribution increased by 1% and 9%, respectively. Furthermore, slight shifts in the binding energy of the C 1s spectra are observed in samples A1, N1 and S1, and may be associated with a change in the environment of carbons within cotton. This change begins in the primary exhaustion stage and would be related to the presence of copper. The surface of cellulosic fibers in water becomes negatively ionized due to carbonyl and hydroxyl groups.^{31, 32} Similarly, in an aqueous solution, the three salts of copper acetate, nitrate, and sulfate form the same aqua-copper (II) ion with two positive charges,^{21, 33} but with different anions. These anions will have an electrostatic barrier to diffuse through the cotton fiber because of the negative charge. Consequently, in the primary exhaustion stage, ionized cellulose and the aqua-copper ion come into contact; due to this interaction, the fabric acquires a yellow-greenish hue (discussed in section 3.1) resistant to domestic washing cycles.³⁴ This resistance suggests the existence of a strong interaction between cotton and copper, probably chemical rather than physical.

The study by Ali *et al.*³⁵ proposed the existence of a strong bond between Cu²⁺ ions and the surface of cotton fabrics metalized with copper, which were previously activated with silver and copper particles. In addition, these authors mention the formation of ionic bonds between the electronegative groups of cotton and the Cu²⁺ ion. Zhang *et al.*³⁶ reported the formation of covalent bonds between a cotton fiber treated with titanium sulfate, urea, and hexadecyl trimethylammonium bromide and titanium dioxide (TiO₂). The authors suggest that TiO₂ reacts with cotton through the hydroxyl group of carbon 6 of cellulose. Also, other authors reported that the essential reaction in treating cellulosic textiles with metal salts is the ion exchange interaction

between carboxylic groups of cellulose and the metal ions.³⁷ From these studies, it is inferred that electronegative groups of cotton form a chemical bond with metal ions. We conclude that there is a chemical interaction between the hydroxyl groups of cotton cellulose and copper. The possible reaction mechanism between these two materials could originate from the replacement of some of the water molecules of the aqua-copper ion by oxygens from the ionized cellulose, which have unpaired pairs of electrons that can form coordinated bonds with metal ions, thus producing a probable copper-cotton complex.

The C 1s spectra of the samples taken after the addition of NaOH, temperature increase to 90 °C, and cooling to 70 °C (A4, N4, and S4) are shown in Figure 5(b). The spectra from cotton have a peak with binding energy around 285.0 eV attributed to the C-C/C-H groups,³⁸ indicating a non-cellulosic origin, such as wax remnants from the cotton itself that are a mixture of hydrocarbons, alcohols, esters, fatty acids, alkanes and glycerides.³⁸⁻⁴⁰ In this study, the addition of NaOH caused an evident reduction in the spectral contribution of the C1 component of cotton. This component, with average binding energy of 284.9 eV, was reduced from 49% in NF to 35% in A4, 29% in N4 and 41% in S4. This decrease may be from elimination of some pre-existing non-cellulosic material in the cotton or could arise from modification of the fiber itself during the secondary exhaustion stage. In contrast, the spectral contribution of C2, with an average energy of 286.8 eV belonging to the C-O bonds,^{39, 41} has risen by 7 to 15% in samples A4, N4 and S4, compared to the NF. Work by Huang *et al.*⁴² show a modified eucalyptus fiber at low-temperature plasma (LPT) within a mixture of air and oxygen, where the intensity of the C2 peak was enhanced due to the LPT treatment that exposed more hydroxyls on the surface of fibers. Therefore, the increase in C2 intensity for A4, N4, and S4 samples should be related to the effect of NaOH, because of the greater presence of hydroxyls on the surface of the cotton fiber. The C3 contribution associated

with O-C-O or C=O bonds at 288.0 eV³⁸⁻⁴⁰ increased intensity by 3% for A4, 5% for N4 and 1% for S4, compared to NF. This increase in intensity could be due to the breaking of C-C, C-H, or C-O bonds that cause the formation of carbonyl or O-C-O groups on the fiber surface.^{38, 42}

Figure 5(c) shows the C 1s spectra of the samples functionalized with CuO_x, obtained after the subsequent processes stage (A5, N5, and S5). The XPS spectra of these samples exhibited changes in the contributions of components C1, C2, and C3 compared to the NF sample. The C1 contribution decreased by 13, 16 and 11% for samples A5, N5 and S5, respectively, while the C2 contributions rose by 9%, 13% and 5%, and the C3 contributions grew by 4%, 3% and 6% for the same samples, respectively. These trends are similar as those seen in samples A4, N4 and S4. This similarity suggests that the C-C/C-H, -C-O and O-C-O/C=O bonds associated with C1, C2 and C3, respectively, present resistance to the effects of subsequent rinsing and neutralization. The XPS results also show that subsequent processes are modifying the carbon atoms on the surface of A5, N5 and S5. The observed decrease in the C1 contribution can be attributed to a reduction in the number of C-C/C-H bonds, possibly due to the breaking of hydrocarbon chains during the rinsing and neutralization processes. Conversely, increases in the C2 and C3 contributions are associated with a rise in the amount of -C-O and O-C-O/C=O bonds, which could indicate the formation of carbonyl or carboxylic groups on the surface of the samples. Overall, the carbon XPS data enhances our understanding of the impact of the latter processes on the surface properties of the functionalized cotton textiles.

Figure 6 shows the Cu 2p XPS spectrum of non-functionalized fabric and fabric functionalized with CuO_x using 2% owf acetate, nitrate, and copper sulfate salts. The Cu 2p peak is composed of Cu 2p1/2 and Cu 2p3/2 doublets along with satellite (Sat) peaks,^{15, 43} which can be seen in all the samples analyzed, except for NF.

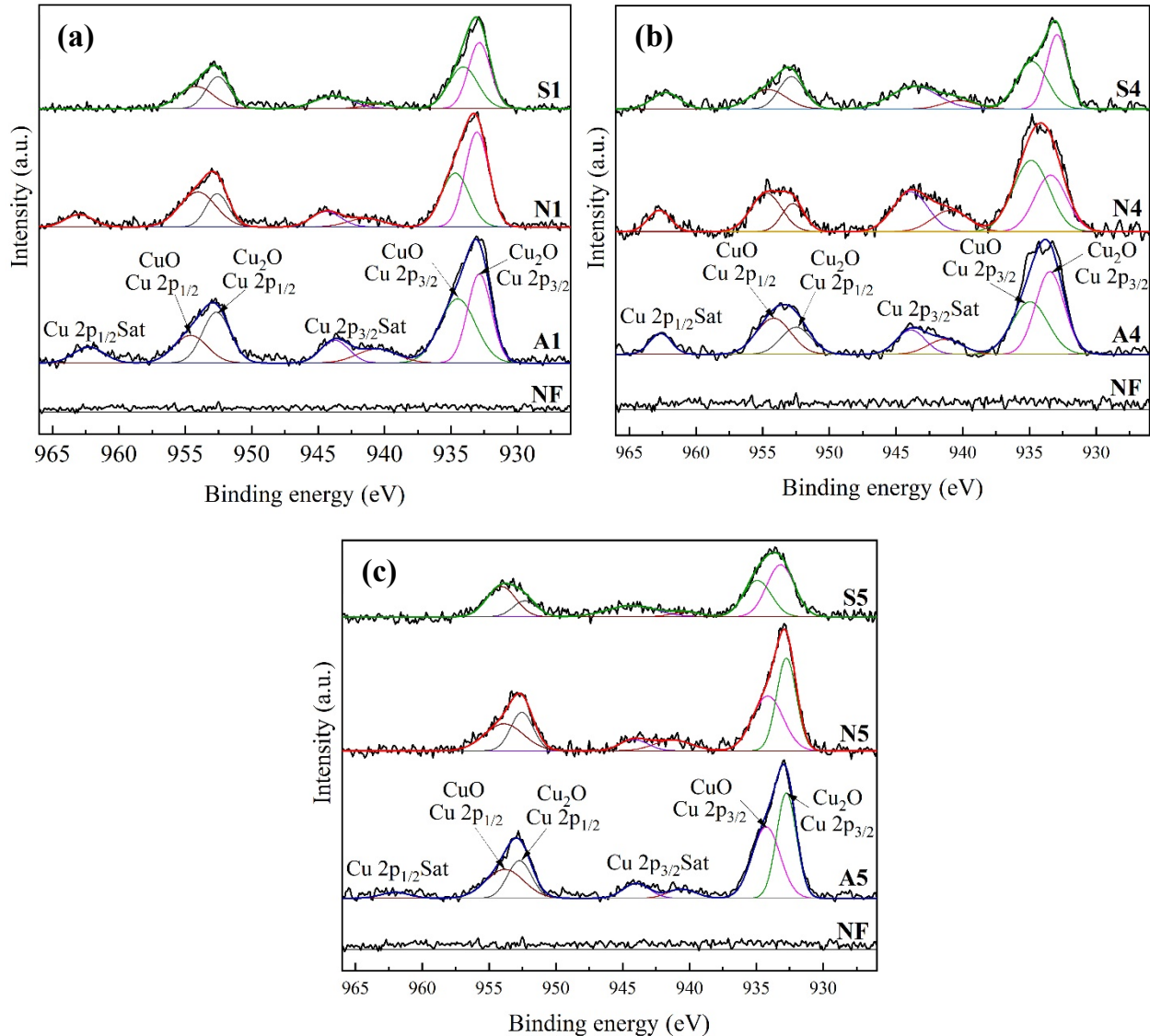


Figure 6. XPS spectra of Cu 2p electrons in non-functionalized fabric and fabrics taken: (a) at 25 °C with copper salts, (b) after the addition of NaOH, temperature increase to 90 °C and cooling to 70 °C, and (c) after functionalization with CuO_x with rinses and neutralization.

The Cu 2p_{3/2} peak deconvolves into two contributions for A1, N1, and S1 (samples taken after primary exhaustion stage, Figure 6(a)). The contribution around 933.4, 933.0, and 932.8 eV for A1, N1, and S1, respectively, is attributed to cuprous ion (Cu¹⁺).^{15, 44} The other contribution is located at 934.9 eV for A1, 936.4 eV for N1, and 934.0 eV for S1, and this is attributed to cupric

ion (Cu^{2+}).^{15, 44, 45} The Cu 2p1/2 also deconvolves into two contributions. The binding energy of 952.4 eV for A1 and 952.5 eV for N1 and S1 corresponds to the contribution of Cu^{1+} , while 954.1 eV for A1 and S1 and 954.0 eV for N1 are attributed to Cu^{2+} .^{15, 43} Copper in its 2+ oxidation state exhibits a Sat peak, which is not observed for copper in a zero or 1+ oxidation state.⁴⁶ In the same spectrum of Figure 6(a), multiple features are observed between 940 and 945 eV and around 962 eV, associated with the peaks for Cu 2p3/2 Sat and Cu 2p1/2 Sat, respectively. Both are assigned to the copper Sat peaks,^{15, 43, 47, 48} suggesting that copper on the cotton surface is mainly found as Cu^{2+} , which is derived from the dissolution of copper salts in water. However, at the end of the primary exhaustion stage, the existence of Cu^{1+} is also apparent in the spectrum.

Cotton textile materials accumulate natural and added impurities during their manufacturing, such as oils and dressings.^{49, 50} These impurities can affect subsequent processes, such as dyeing or printing, so prior cleaning by de-sizing, scouring, and bleaching is necessary.⁵⁰⁻⁵² Mitchell *et al.* compared XPS spectra of C 1s between bleached and scouring cotton, finding similarities in the spectral intensity of 285.0 eV, specifically in the C1 (-C-C, -C-H) region, which suggests the persistent presence of some organic material in cotton fibers. Based on these results, the authors demonstrated that after the bleaching and scouring process there are still residues of non-cellulosic material on the surface of cotton fibers, which consist of a complex mixture of alcohols, esters, fatty acids, alkanes and glycerides. Therefore, it is possible that the fabric used in this research contains non-cellulosic residues and remains of chemicals from the bleaching process mentioned in section 2.1, which could act as reducing agents. For this reason, the contributions of Cu^{1+} observed in the XPS spectrum of A1, N1, and S1 samples could be associated with the reduction of Cu^{2+} in primary exhaustion.

The Cu 2p spectra of A4, N4, and S4 samples taken after the addition of NaOH, temperature increase to 90 °C and cooling to 70 °C, are presented in Figure 6(b). In the 931 to 938 eV region, contributions from A4, N4, and S4 were observed at 932.7, 933.4, and 932.9 eV, respectively. These peaks can be assigned to Cu(I) 2p3/2.⁴³ Peaks close to 934.2, 934.1, and 934.8 eV are also apparent in the same samples, which could correspond to Cu(II) 2p3/2.^{15, 53} The spectra shows peaks at energies of 952.7 eV for A4 and N4, and 952.8 eV for S4, which could be associated with Cu(I) 2p1/2.⁴³ Other binding energies were also observed at 953.8 eV for A4, 954.7 eV for N4 and 954.6 eV for S4, which could correspond to Cu(II) 2p1/2.⁴³ Likewise, an increase in the intensity of the Sat peaks located between the binding energy regions of 940-944 eV and 960-965 eV can be seen, when compared to the Sat peaks of A1, N1 and S1. This increase suggests that Cu²⁺ is not only present as CuO but also as Cu(OH)₂.⁵⁴ OH⁻ ions derived from the ionization of NaOH during the secondary exhaustion stage can pull H⁺ ions from water molecules present in the copper-cotton complex that was probably formed in the primary exhaustion stage.⁵⁵ This hypothesis was suggested in the discussion of Figure 5(a). After the removal of H⁺, copper hydroxide (Cu(OH)₂) would form in the fabric, and subsequently, by increasing the temperature to 90 °C for 20 minutes, the Cu(OH)₂ can be transformed into CuO, which is then partially reduced to Cu₂O. Consequently, a mixture of copper oxides and copper hydroxide remanent would be found on the surface of A4, N4, and S4 samples.

Figure 6(c) shows the XPS spectra of the A5, N5, and S5 samples obtained after rinsing and neutralizing. It can be seen that the Cu 2p doublet peaks remain in these samples. For Cu¹⁺, peaks were found between 932.7 to 933.1 eV that can be assigned to Cu 2p3/2 and peaks between 952.2 to 952.6 eV for Cu 2p1/2.^{43, 47} In the case of Cu²⁺, the peaks observed in the range of 934.1-943.9 eV and 953.8-954.6 eV may correspond to the binding energies of Cu 2p3/2 and Cu 2p1/2,

respectively.^{43, 47} In addition, a decrease in the intensity of the Sat peaks placed between the binding energies of 940 to 945 eV is observed in the three samples examined, while the peak close to 962.2 eV practically disappears in samples N5 and S5. This behavior could be related to eliminating the remaining Cu(OH)₂ on the fabric surface during the rinses with hot and cold water, followed by pH neutralization. Therefore, XPS analyses in the Cu 2p region revealed that, after the functionalization process with copper salts, the cotton fabric presented peaks attributable to Cu²⁺ and Cu¹⁺ ions. These results suggest the formation of CuO, Cu₂O, and possibly small amounts of Cu(OH)₂.

Samples A5, N5, and S5 were selected for complementary characterizations. These samples represent the final product of the functionalization process of cotton fabric with CuO_x. We used SAED, TOF-SIMS, and SEM to determine the morphology and structure of copper-functionalized fabric.

The SAED patterns were used to study the crystallinity of the CuO_x particles. Figure 7 shows the patterns acquired for the functionalized fabrics; for each raw set, images and patterns belongs to A5, N5, and S5. In the first column, the morphology of the particles can be seen; in the case of CuO, approximately 10nm particles are agglomerated, as shown in Figure 7(b). In contrast, the Cu₂O particles are more dispersed, as shown in Figures 7(a) and 7(c); the particles are generally aggregated and are approximately 10 nm in diameter. The reflections apparent in all SAED patterns were indexed as polycrystalline, and arise from multiple crystals in different orientations. The images in the second column (Figures 7(d), 7(e), and 7(f)) show SAED patterns, which were indexed to the Cu₂O crystal phase using the card from the database of JCPDS # 00-005-0667 cuprite system with cubic crystal system. The images in the third column (Figures 7(g), 7(h), and 7(i)) show SAED patterns, which, in this case, were indexed to the CuO crystal phase by card from

the database of JCPDS # 00-045-0937 tenorite system with monoclinic crystal system. These tiny (≈ 10 nm) CuO_x nanoparticles are crystals, and the copper oxide phases (CuO and Cu_2O) are present for all samples; this confirms our XPS results discussed in the previous section that indicate the presence of both Cu oxide phases.

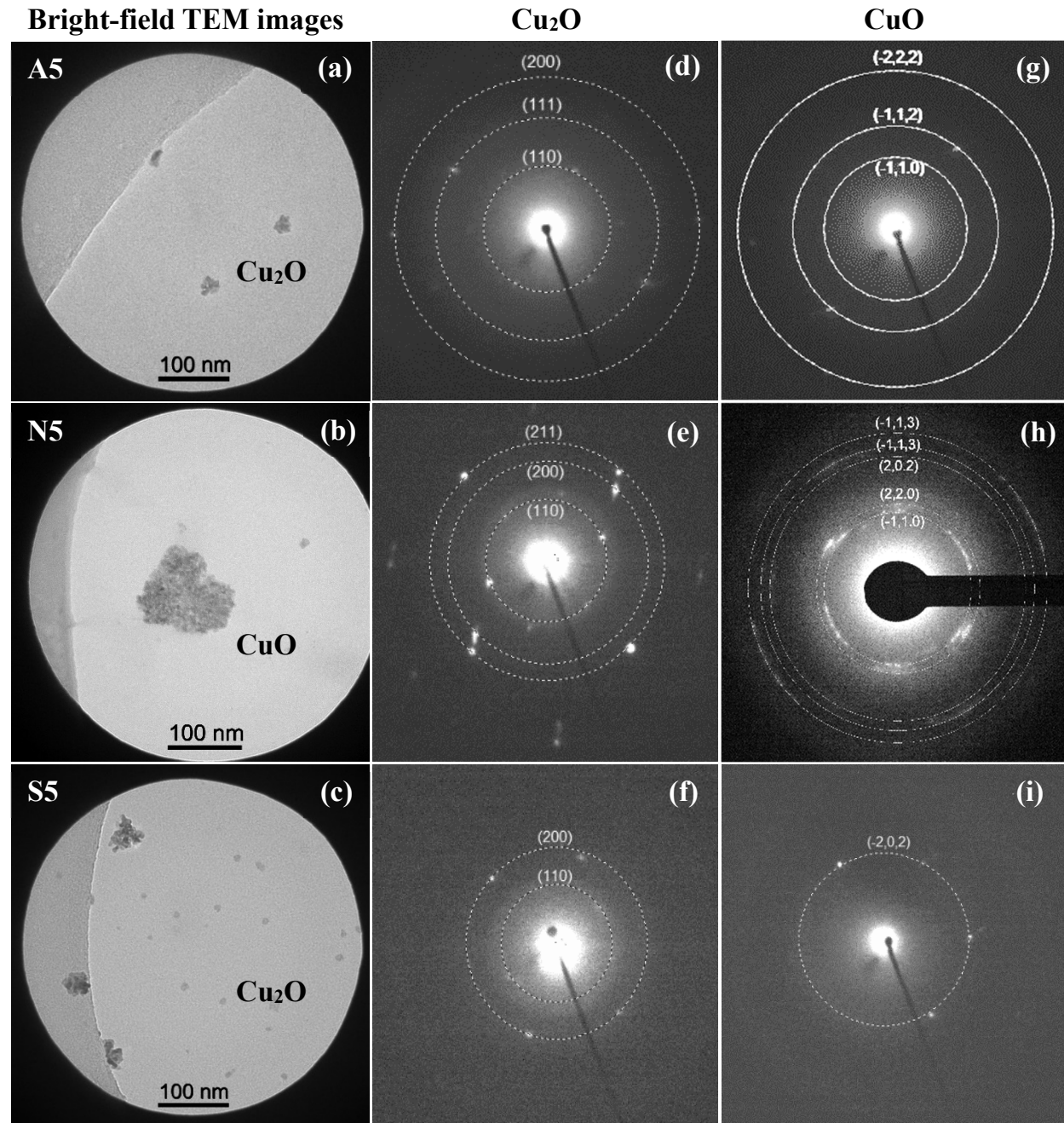


Figure 7. TEM images of fabrics functionalized with CuO_x after the subsequent processes stage (A5, N5, and S5) (a, b, c) and the SAED pattern of Cu_2O (d, e, f) and CuO (g, h, i).

Figure 8 shows the TOF-SIMS positive ion mass spectra of the non-functionalized fabric and the fabric functionalized with CuO_x after the last processing stage (A5, N5, and S5). Figure 8(a) shows that the mass spectra from NF, A5, N5, and S5, which mostly exhibit typical patterns associated with cellulose.^{38, 56} In Figure 8(b), A5, N5, and S5 also exhibit a peak at m/z 62.929 that varies with each fabric sample and that is indicative of the presence of copper.^{57, 58} This peak is absent in spectrum from NF, as expected. Copper-organic fragments were also detected in other regions of the secondary ion spectra from A5, N5, and S5, specifically in the m/z ranges of 92–93 and 106–107, as illustrated in Figure 8(c). This suggests a high probability of Cu grafting in the functionalized cotton fabric, as suggested by XPS. However, uncovering the factors that govern the formation of secondary ions from fabric functionalized with CuO_x is complex and will require further work.

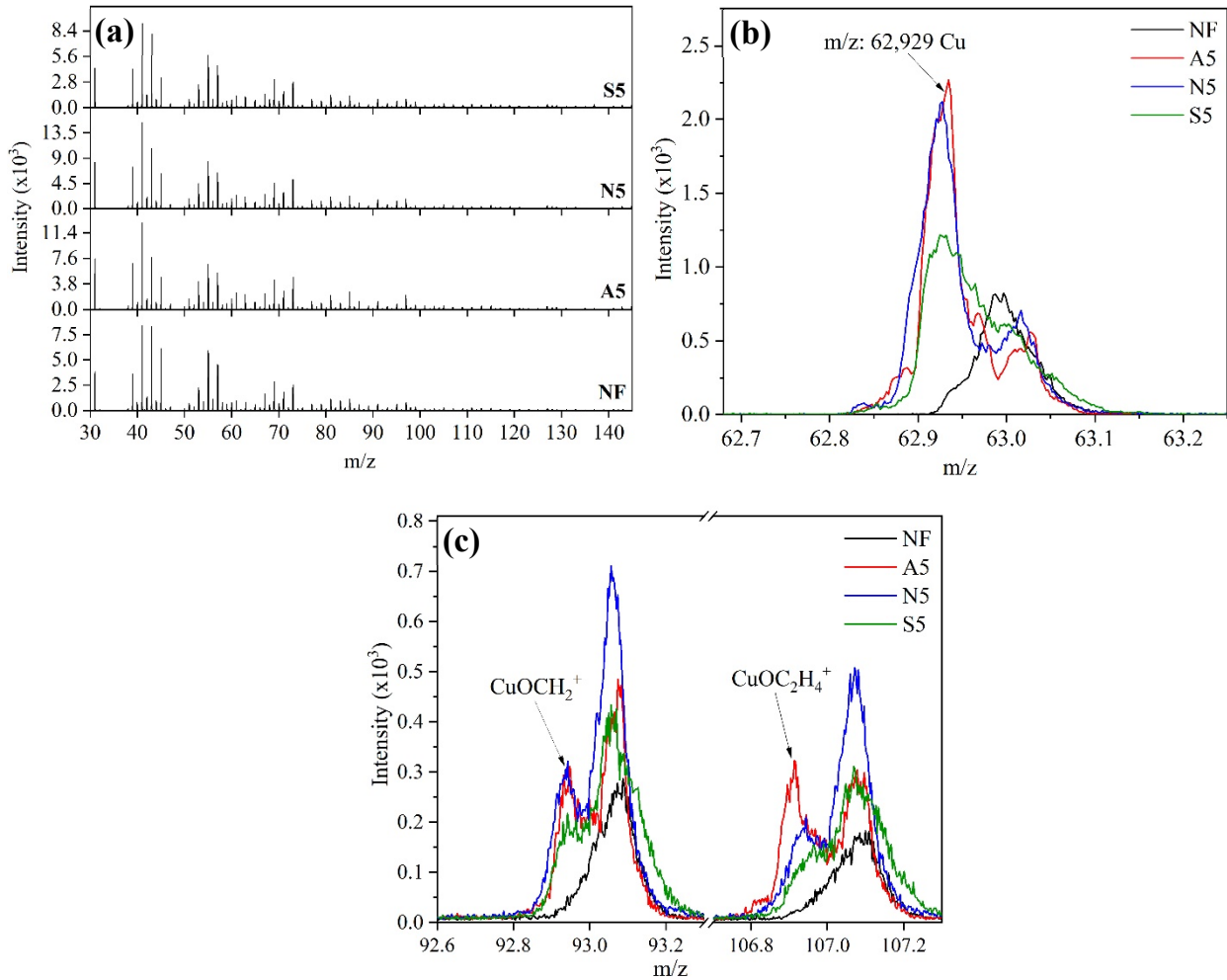


Figure 8. Positive ion TOF-SIMS spectrum of the non-functionalized fabric and fabrics functionalized with CuO_x after subsequent processes stage (A5, N5, and S5) in the m/z ranges of: (a) 30 – 140, (b) 62.7 – 63.2, and (c) 92.6 – 107.2.

We used SEM to examine the distribution and morphology of CuO_x on cotton fabric surfaces. Micrographs of non-functionalized and functionalized fabrics with CuO_x after latter processing stages (A5, N5, and S5) are illustrated in Figures 9. Figure 9(a) shows the intrinsic morphology of the non-functionalized cotton fiber. A clean surface is seen with parallel grooves that resemble

folds.³¹ These folds are observed more clearly in Figure 9(b), in which the cellulose microfibrils that are components of the secondary wall of cotton fiber are also apparent, as crisscrossed threads that follow different directions on the fiber surface.⁵⁹

In contrast to the micrographs from non-functionalized fabric, particles are apparent on the cotton fiber surface for all samples obtained from the salts of copper acetate (Figure 9(c)), nitrate (Figure 9(e)) and sulfate (Figure 9(g)). By increasing the magnification from 25,000 to 120,000 times, we can observe how these particles are aggregated into irregular shapes with different sizes, where some are located between the folds of the cotton fiber (See Figures 9 (d), (f), and (h)). These images confirm the presence of CuO_x particles on the functionalized fabric using our various copper salt sources.

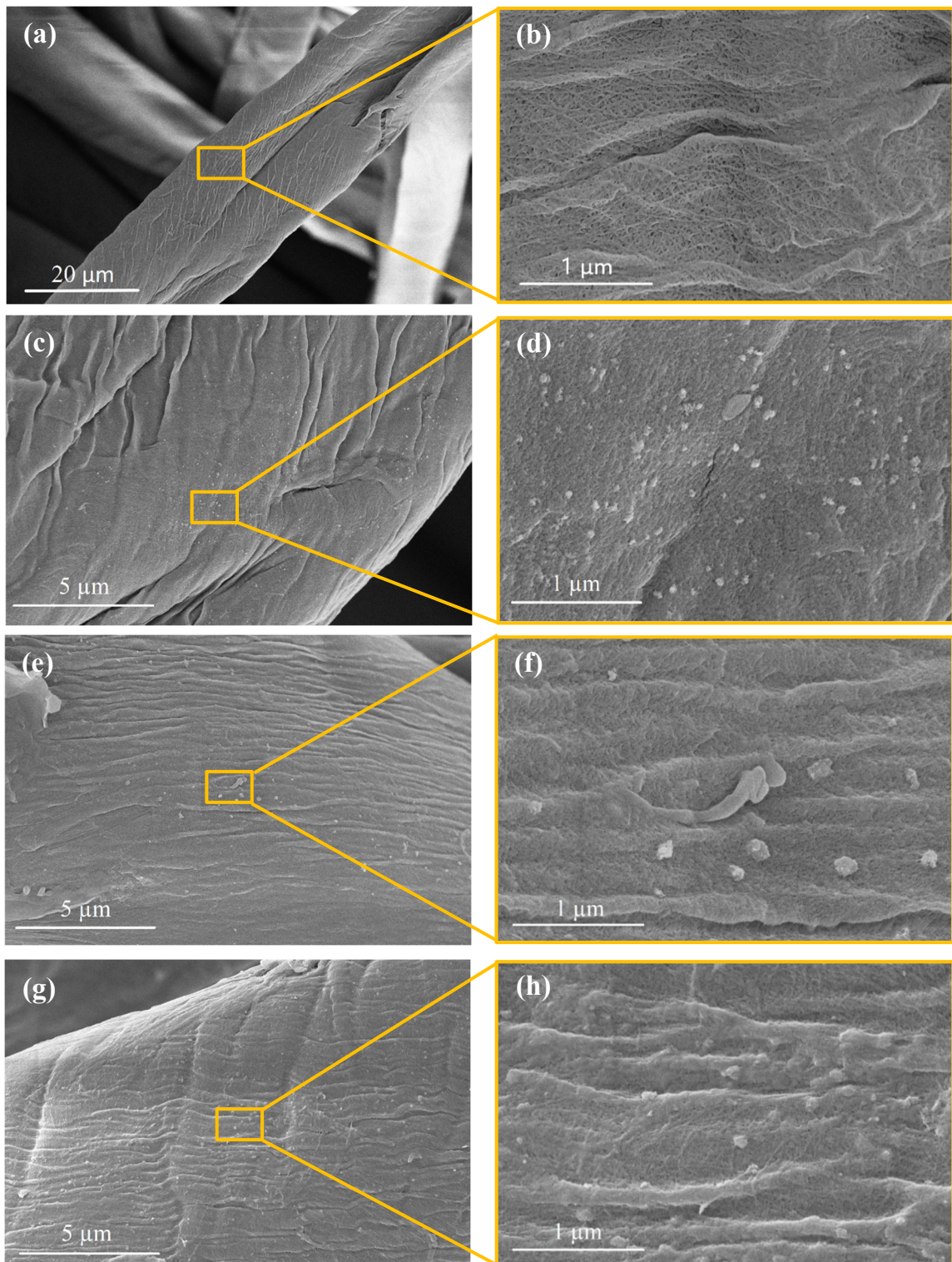


Figure 9. SEM micrographs of the non-functionalized fabric at magnifications of (a) 5000x and (b) 120,000x, and of the fabric functionalized with CuO_x using copper: acetate (c, d; A5); nitrate (e, f; N5); and sulfate (g, h; S5) at 25,000x and 120,000x.

3.3. Antibacterial evaluation

The percentage of bacterial reduction against the strains *E. coli* (ATCC 25922) and *P. aeruginosa* (ATCC 10145) for the non-functionalized and functionalized fabrics with CuO_x after the subsequent processes stage (A5, N5, and S5) are shown in Figure 10(a). The NF fabric experienced a decrease in bacterial growth of 41.8% for *E. coli* and 20.1% for *P. aeruginosa*. These reductions could be attributed to possible pre-existing adventitious contamination of the cotton that inhibits bacterial growth. Furthermore, these percentages were lower than those obtained in fabrics functionalized with CuO_x. In particular, A5, N5, and S5 samples demonstrated an inhibition of bacterial growth for both strains by 99.99%. According to the literature, the potential mechanism behind the antimicrobial activity of textile materials functionalized with CuO_x, especially at the nanometric level, begins with the adsorption of bacteria on the fabric's surface.^{60, 61} In this condition, the antibacterial activity could be attributed to three possible mechanisms: the direct contact of CuO nanoparticles with bacteria, the release of copper ions and the production of reactive oxygen species (ROS).⁴

Figure 10(b-i) shows the bacterial count in Petri dishes of the two bacterial strains. In Figures 10(b) and 10(f), the presence of colonies can be visualized after 1 h of contact with the NF sample. The bacterial counts were 189×10^4 and 376×10^4 CFU/ml for *E. coli* and *P. aeruginosa*. Figures 10(c), (d), (e), (g), (h), and (i) represent the dishes that were seeded with 100 μ l of each bacterial dilution in contact with the A5, N5, and S5 fabric samples. The absence of growth can be observed in both

strains, suggesting the effectiveness of fabrics functionalized with CuO_x inhibit bacterial development.^{62, 63} This is due to the antimicrobial properties of CuO and Cu₂O.^{17, 64} Therefore, these fabrics offer effective antibacterial properties against Gram-negative bacterial strains, which underlines their potential in antimicrobial applications.

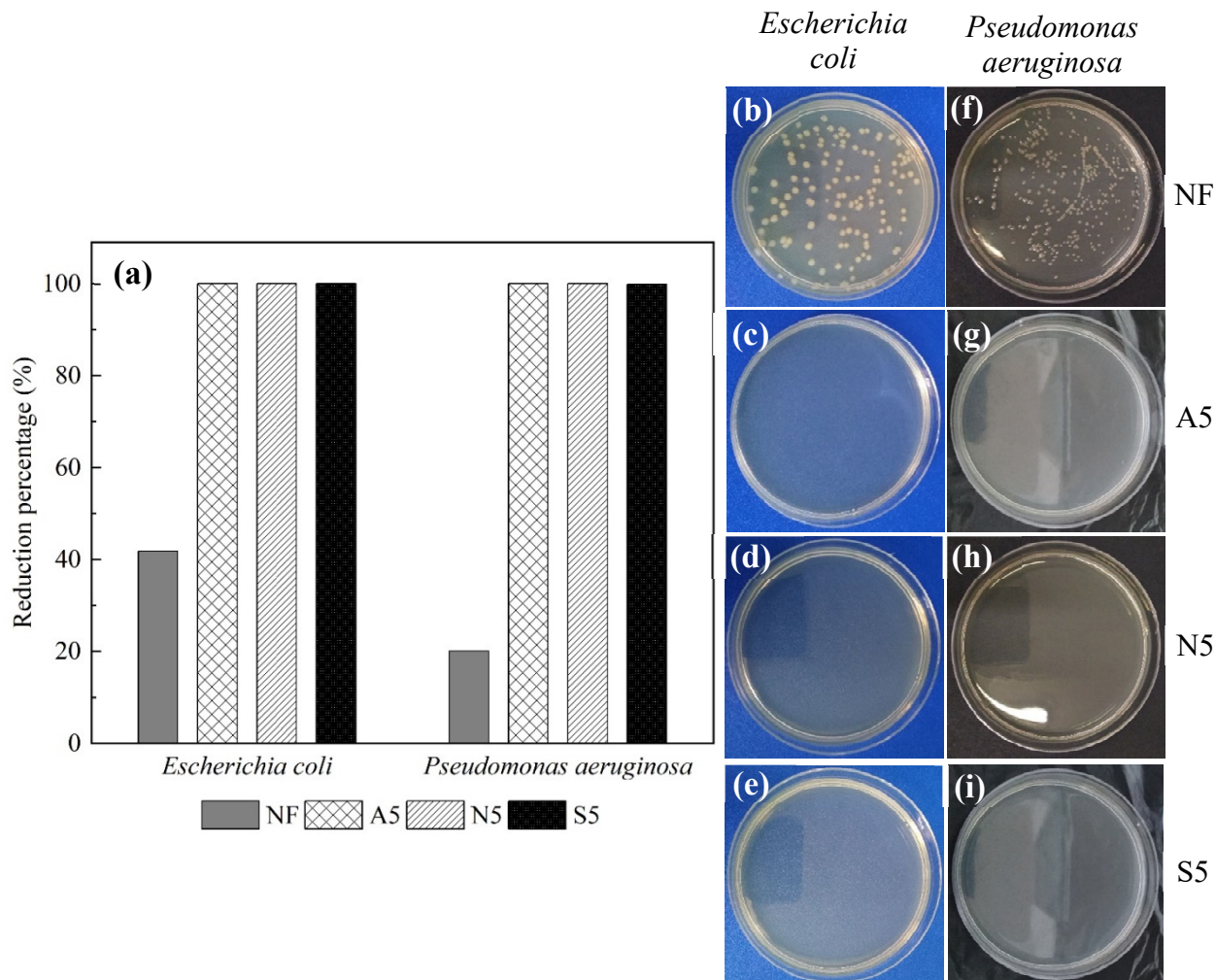


Figure 10. Percentage of bacterial reduction (a), and count of *E. coli* (ATCC 25922) and *P. aeruginosa* (ATCC 10145) strains after 1 h contact time with: non-functionalized (b, f); and functionalized fabrics with CuO_x for A5 (c, g), N5 (d, h) and S5 (e, i).

4. CONCLUSIONS

Antimicrobial cotton fabrics have been manufactured through exhaustion dyeing, using 2% owf of copper source salts based on acetate, nitrate, and sulfate. The colorimetric characteristic of the non-functionalized fabric was a yellow hue and luminous, while after the functionalization process, it turned greenish and finally reddish brown due to the presence of CuO_x . The chemical composition of functionalized cotton fabric was determined by ICP chemical analysis, which showed, in general, that the copper content had significantly increased to 40, 32, and 27 wt. % of the bath concentration in A5, N5, and S5, respectively. These values are in comparison to the initial value of non-functionalized fabric. The XPS results suggest a chemical interaction between hydroxyl groups of cellulose and copper oxide, whose possible reaction route could have originated from replacing water molecules in copper (II) hydrated complexes with lone pairs of electrons from the oxygen atom of cellulose, forming a copper-cotton complex. Also, XPS analyses in the Cu 2p region showed that after the functionalization process with copper salts, the cotton fabric showed characteristic peaks of Cu^{2+} and Cu^{1+} ions, indicating the formation of CuO , Cu_2O phases and possible traces of $\text{Cu}(\text{OH})_2$. The phases were corroborated by SAED. Cu_2O was indexed in the cuprite system and CuO in tenorite system. Furthermore, copper-organic fragments were detected functionalized fabric by TOF-SIMS analysis. Morphological characterization shows that CuO_x particles are agglomerated in various shapes and sizes, and they are distributed randomly on the cotton fiber surface. Finally, fabrics functionalized with CuO_x presented an effective antibacterial property against both Gram-negative strains, highlighting their potential in antimicrobial applications.

AUTHOR INFORMATION

Corresponding Author

*Mónica M. Gómez – Faculty of Sciencead de , Universidad Nacional de Ingeniería, Av. Túpac Amaru 210, Lima 15333, Peru; orcid.org/0000-0003-0990-0593; Phone: +51 948458401; Email: mgomez@uni.edu.pe

Author Contributions

The manuscript was written with contributions from all authors. They have approved the final version of the manuscript.

Funding Sources

This research was funded by the National Council of Science Technology and Technology Innovation of Peru (CONCYTEC)/PROCIENCIA Program, according to contract N°PE501084249-2023-PROCIENCIA. J.G.S. and E.D.G. acknowledge financial support from the U.S. National Science Foundation under Award DMR- 1905550. J.G.S. acknowledges financial support from the U.S. National Science Foundation Graduate Research Fellowship Program (Award DGE-1255832).

Notes

The authors declare no competing financial interest.

ACKNOWLEDGMENT

Luz E. Román thanks the CONCYTEC/PROCIENCIA Program (N°PE501084249-2023-PROCIENCIA) for the postdoctoral fellowship. We also sincerely thank Professor Dora Maurtua, Faculty of Science and Philosophy, Universidad Peruana Cayetano Heredia, and Professor Gerardo

Cruz and Liliana Solis at Facultad de Ciencias Agrarias, Universidad Nacional de Tumbes, for the antibacterial evaluation.

REFERENCES

- (1) Mallakpour, S.; Azadi, E.; Hussain, C. M. Recent Breakthroughs of Antibacterial and Antiviral Protective Polymeric Materials During Covid-19 Pandemic and after Pandemic: Coating, Packaging, and Textile Applications. *Curr. Opin. Colloid Interface Sci.* **2021**, *55*, 101480.
- (2) Chen, W.; Chen, J.; Li, L.; Wang, X.; Wei, Q.; Ghiladi, R. A.; Wang, Q. Wool/Acrylic Blended Fabrics as Next-Generation Photodynamic Antimicrobial Materials. *ACS Appl. Mater. Interfaces.* **2019**, *11*, 29557-29568.
- (3) Mahltig, B. Cellulosic-Based Composite Fibers. In *Inorganic and Composite Fibers: Production, Properties, and Applications*, Woodhead Publishing; 2018; pp. 277-301. DOI: 10.1016/b978-0-08-102228-3.00013-x
- (4) Román, L. E.; Gomez, E. D.; Solís, J.; Gómez, M. Antibacterial Cotton Fabric Functionalized with Copper Oxide Nanoparticles. *Molecules.* **2020**, *25*, 5802.
- (5) Perelshtein, I.; Levi, I.; Perkas, N.; Pollak, A.; Gedanken, A. CuO-Coated Antibacterial and Antiviral Car Air-Conditioning Filters. *ACS Appl. Mater. Interfaces.* **2022**, *14*, 24850-24855.
- (6) Mahdy, N. K.; El-Sayed, M.; Al-Mofty, S. E.; Mohamed, A.; Karaly, A. H.; El-Naggar, M. E.; Nageh, H.; Sarhan, W. A.; El-Said Azzazy, H. M. Toward Scaling up the Production of Metal Oxide Nanoparticles for Application on Washable Antimicrobial Cotton Fabrics. *ACS Omega.* **2022**, *7*, 38942-38956.

(7) Subhapriya, S.; Gomathipriya, P. Green Synthesis of Titanium Dioxide (TiO_2) Nanoparticles by *Trigonella foenum-graecum* Extract and its Antimicrobial Properties. *Microb. Pathog.* **2018**, *116*, 215-220.

(8) Ghatage, M. M.; Mane, P. A.; Gambhir, R. P.; Parkhe, V. S.; Kamble, P. A.; Lokhande, C. D.; Tiwari, A. P. Green Synthesis of Silver Nanoparticles Via Aloe Barbadensis Miller Leaves: Anticancer, Antioxidative, Antimicrobial and Photocatalytic Properties. *Appl. Surf. Sci. Adv.* **2023**, *16*, 100426.

(9) Oladeji, A. V.; Courtney, J. M.; Rees, N. V. Copper Deposition on Metallic and Non-Metallic Single Particles Via Impact Electrochemistry. *Electrochim. Acta* **2022**, *405*, 139838.

(10) Masoumi, Z.; Tayebi, M.; Tayebi, M.; Masoumi Lari, S. A.; Sewwandi, N.; Seo, B.; Lim, C. S.; Kim, H. G.; Kyung, D. Electrocatalytic Reactions for Converting CO_2 to Value-Added Products: Recent Progress and Emerging Trends. *Int. J. Mol. Sci.* **2023**, *24*.

(11) Gao, F.; Wang, X.; Wu, D. Design and Fabrication of Bifunctional Microcapsules for Solar Thermal Energy Storage and Solar Photocatalysis by Encapsulating Paraffin Phase Change Material into Cuprous Oxide. *Sol. Energy Mater. Sol. Cells.* **2017**, *168*, 146-164.

(12) Moradi, O.; Alizadeh, H.; Sedaghat, S. Removal of Pharmaceuticals (Diclofenac and Amoxicillin) by Maltodextrin/Reduced Graphene and Maltodextrin/Reduced Graphene/Copper Oxide Nanocomposites. *Chemosphere* **2022**, *299*, 134435.

(13) Hillyer, M. B.; Nam, S.; Condon, B. D. Intrafibrillar Dispersion of Cuprous Oxide (Cu_2O) Nanoflowers within Cotton Cellulose Fabrics for Permanent Antibacterial, Antifungal and Antiviral Activity. *Molecules* **2022**, *27*.

(14) Prakash, J.; Krishna, S. B. N.; Kumar, P.; Kumar, V.; Ghosh, K. S.; Swart, H. C.; Bellucci, S.; Cho, J. Recent Advances on Metal Oxide Based Nano-Photocatalysts as Potential Antibacterial and Antiviral Agents. *Catalysts*. **2022**, *12*, 1047.

(15) Shaheen, T. I.; Fouda, A.; Salem, S. S. Integration of Cotton Fabrics with Biosynthesized CuO Nanoparticles for Bactericidal Activity in the Terms of their Cytotoxicity Assessment. *Ind. Eng. Chem. Res.* **2021**, *60*, 1553-1563.

(16) Bahtiyari, M. İ.; Körlü, A.; Akca, C. Antimicrobial Textiles for the Healthcare System. In *Advances in Healthcare and Protective Textiles*, Woodhead Publishing; 2023; pp. 57-91. DOI: 10.1016/b978-0-323-91188-7.00013-3

(17) El-Nahhal, I. M.; Salem, J.; Kodeh, F. S.; Elmanama, A.; Anbar, R. CuO-NPs, CuO-Ag Nanocomposite and Cu(II)-Curcumin Complex Coated Cotton/Starched Cotton Antimicrobial Materials. *Mater. Chem. Phys.* **2022**, *285*, 126099.

(18) Zarbaf, D.; Montazer, M.; Sadeghian Maryan, A. *In-situ* Synthesis of Nano-Copper on Denim Garment along with Nano-Clay for Antibacterial and Decoloration Purposes. *Cellulose*. **2017**, *24*, 4083-4095.

(19) Villalva, C. Incorporación de nanopartículas de óxido de cobre en tejidos de algodón para mejorar la solidez al sudor a partir de diferentes métodos textiles: agotamiento, impregnación, agotamiento-impregnación. Bachelor Dissertation, Universidad Nacional de Ingeniería, Lima, Peru, 2021.

(20) Chakraborty, J. N. Introduction to Dyeing of Textiles. In *Fundamentals and Practices in Colouration of Textiles*, Woodhead Publishing India; 2010; pp. 1-10. DOI: 10.1533/9780857092823.1

(21) Cotton, F. A.; Wilkinson, G.; Murillo, C. A.; Bochmann, M. *Advanced inorganic chemistry*; John Wiley & Sons Inc, 1999.

(22) Huang, M.-L.; Cai, Z.; Wu, Y.-Z.; Lu, S.-G.; Luo, B.-S.; Li, Y.-H. Metallic coloration on polyester fabric with sputtered copper and copper oxides films. *Vacuum*. **2020**, 178, 109489.

(23) Cegarra, J. S. *Fundamentos de la Maquinaria de Tintorería*; Universidad Politécnica de Cataluña, 1987.

(24) Clark, M. *Handbook of Textile and Industrial Dyeing Volume 2: Applications of Dyes*; Woodhead Publishing Limited, 2011.

(25) Ruiz-Caldas, M.-X.; Carlsson, J.; Sadiktsis, I.; Jaworski, A.; Nilsson, U.; Mathew, A. P. Cellulose Nanocrystals from Postconsumer Cotton and Blended Fabrics: A Study on their Properties, Chemical Composition, and Process Efficiency. *ACS Sustainable Chem. Eng.* **2022**, 10, 3787-3798.

(26) Wakelyn, P. J.; French, A. D. *Cotton Fiber Chemistry and Technology*; Taylor & Francis Group, LLC, 2006.

(27) Nam, S.; Hillyer, M. B.; Condon, B. D.; Lum, J. S.; Richards, M. N.; Zhang, Q. Silver Nanoparticle-Infused Cotton Fiber: Durability and Aqueous Release of Silver in Laundry Water. *J. Agric. Food Chem.* **2020**, 68, 13231-13240.

(28) Riaz, S.; Ashraf, M.; Aziz, H.; Younus, A.; Umair, M.; Salam, A.; Iqbal, K.; Hussain, M. T.; Hussain, T. Cationization of TiO₂ Nanoparticles to Develop Highly Durable Multifunctional Cotton Fabric. *Mater. Chem. Phys.* **2022**, *278*, 125573.

(29) Yu, M.; Wang, Q.; Yang, W.; Xu, Y.; Zhang, M.; Deng, Q.; Liu, G. Facile Fabrication of Magnetic, Durable and Superhydrophobic Cotton for Efficient Oil/Water Separation. *Polymers*. **2019**, *11*, 442.

(30) Pertile, R. A. N.; Andrade, F. K.; Alves, C.; Gama, M. Surface Modification of Bacterial Cellulose by Nitrogen-Containing Plasma for Improved Interaction with Cells. *Carbohydr. Polym.* **2010**, *82*, 692-698.

(31) Gordon, S.; Hsieh, Y. L. *Cotton: Science and technology*; Woodhead Publishing, 2007.

(32) Ribitsch, V.; Stana-Kleinscheck, K. Characterizing Textile Fiber Surfaces with Streaming Potential Measurements. *Text. Res. J.* **1998**, *68*, 701-707.

(33) Brown, T. L.; LeMay, H. E.; Bursten, B. E.; Murphy, C. J.; Woodward, P. M. *Chemistry: The Central Science*; Pearson Prentice Hall, 2012.

(34) Román, L. E.; Amézquita, M. J.; Uribe, C. L.; Maurtua, D. J.; Costa, S. A.; Costa, S. M.; Keiski, R.; Solís, J. L.; Gómez, M. M. *In Situ* Growth of CuO Nanoparticles onto Cotton Textiles. *Adv. Nat. Sci.: Nanosci. Nanotechnol.* **2020**, *11*, 025009.

(35) Ali, A.; Baheti, V.; Vik, M.; Militky, J. Copper Electroless Plating of Cotton Fabrics after Surface Activation with Deposition of Silver and Copper Nanoparticles. *J. Phys. Chem. Solids*. **2020**, *137*, 109181.

(36) Zhang, H.; Zhu, L.; Sun, R. Structure and Properties of Cotton Fibers Modified with Titanium Sulfate and Urea Under Hydrothermal Conditions. *J. Eng. Fibers Fabr.* **2014**, *9*, 67-75.

(37) Emam, H. E. Generic Strategies for Functionalization of Cellulosic Textiles with Metal Salts. *Cellulose*. **2019**, *26*, 1431-1447.

(38) Mitchell, R.; Carr, C. M.; Parfitt, M.; Vickerman, J. C.; Jones, C. Surface Chemical Analysis of Raw Cotton Fibres and Associated Materials. *Cellulose*. **2005**, *12*, 629-639.

(39) Yang, S.; Chen, L.; Liu, S.; Hou, W.; Zhu, J.; Zhao, P.; Zhang, Q. Facile and sustainable fabrication of high-performance cellulose sponge from cotton for oil-in-water emulsion separation. *J. Hazard. Mater.* **2021**, *408*, 124408.

(40) Milošević, M.; Radoičić, M.; Saponjic, Z.; Nunney, T.; Deeks, C.; Lazić, V.; Mitrić, M.; Radetić, T.; Radetić, M. In situ photoreduction of Ag^+ -ions by TiO_2 nanoparticles deposited on cotton and cotton/PET fabrics. *Cellulose*. **2014**, *21*, 3781–3795.

(41) Huang, Z.; Wu, P.; Yin, Y.; Zhou, X.; Fu, L.; Wang, L.; Chen, S.; Tang, X. Preparation of pyridine-modified cotton fibers for anionic dye treatment. *React. Funct. Polym.* **2022**, *172*, 105155.

(42) Huang, C.; Zhao, Y.; Liu, Y.; Chen, Y.; Li, C.; Li, Z. Surface characterization of plasma-treated eucalyptus alkaline peroxide mechanical pulp using electronic spectroscopy chemical analysis and atomic force microscopy. *BioResources*. **2018**, *13*, 3500-3510.

(43) Singh, B. K.; Shaikh, A.; Dusane, R. O.; Parida, S. Copper Oxide Nanosheets and Nanowires Grown by One-Step Linear Sweep Voltammetry for Supercapacitor Application. *J. Energy Storage*. **2020**, *31*, 101631.

(44) Jurado-López, B.; Vieira, R. S.; Rabelo, R. B.; Beppu, M. M.; Casado, J.; Rodríguez-Castellón, E. Formation of Complexes Between Functionalized Chitosan Membranes and Copper: A Study by Angle Resolved XPS. *Mater. Chem. Phys.* **2017**, *185*, 152-161.

(45) Siddiqui, H.; Parra, M. R.; Pandey, P.; Qureshi, M. S.; Haque, F. Z. Utility of Copper Oxide Nanoparticles (CuO-NPs) as Efficient Electron Donor Material in Bulk-Heterojunction Solar Cells with Enhanced Power Conversion Efficiency. *J. Sci.: Adv. Mater. Devices*. **2020**, *5*, 104-110.

(46) Faraldos, M.; Goberna, C. *Técnicas de análisis y caracterización de materiales*; Consejo Superior de Investigaciones Científicas, 2011.

(47) Errokh, A.; Ferraria, A. M.; Conceicao, D. S.; Vieira Ferreira, L. F.; Botelho do Rego, A. M.; Rei Vilar, M.; Boufi, S. Controlled Growth of Cu₂O Nanoparticles Bound to Cotton Fibres. *Carbohydr. Polym.* **2016**, *141*, 229-237.

(48) Yang, W.; Wang, J.; Ma, W.; Dong, C.; Cheng, G.; Zhang, Z. Free-standing CuO Nanoflake Arrays Coated Cu Foam for Advanced Lithium Ion Battery Anodes. *J. Power Sources*. **2016**, *333*, 88-98.

(49) Gandhi, K. L. *Woven textiles: Principles, technologies and applications*; Woodhead Publishing, 2020.

(50) Clark, M. *Handbook of textile and industrial dyeing. Volumen 1: Principles, processes and types of dyes*; Woodhead Publishing, 2011.

(51) Nawab, Y. *Textile Engineering*; Gruyter Textbook, 2016.

(52) Salem, V. *Tingimento têxtil: fibras, conceitos e tecnologias*; Blucher: Golden Tecnologia, 2010.

(53) Biesinger, M. C. Advanced Analysis of Copper X-Ray Photoelectron Spectra. *Surf. Interface Anal.* **2017**, *49*, 1325-1334.

(54) Mongioví, C.; Crini, G.; Gabrion, X.; Placet, V.; Blondeau-Patissier, V.; Krystianiak, A.; Durand, S.; Beaugrand, J.; Dorlando, A.; Rivard, C.; Gautier, L.; Ribeiro, A. R. L.; Lacalamita, D.; Martel, B.; Staelens, J.-N.; Ivanovska, A.; Kostić, M.; Heintz, O.; Bradu, C.; Raschetti, M.; Morin-Crini, N. Revealing the Adsorption Mechanism of Copper on Hemp-Based Materials through EDX, Nano-CT, XPS, FTIR, Raman, and XANES Characterization Techniques. *Chem. Eng. J. Adv.* **2022**, *10*, 100282.

(55) *Chemguide Home Page. Inorganic Chemistry. Transition Metal. Copper.* <https://www.chemguide.co.uk/inorganic/transition/copper.html> (accessed 2024-02-14).

(56) Kalaskar, D. M.; Ulijn, R. V.; Gough, J. E.; Alexander, M. R.; Scurr, D. J.; Sampson, W. W.; Eichhorn, S. J. Characterisation of Amino Acid Modified Cellulose Surfaces Using ToF-SIMS and XPS. *Cellulose*. **2010**, *17*, 747-756.

(57) Chauhan, D. S.; Quraishi, M. A.; Carrière, C.; Seyeux, A.; Marcus, P.; Singh, A. Electrochemical, ToF-SIMS and Computational Studies of 4-amino-5-methyl-4H-1,2,4-triazole-3-thiol as a Novel Corrosion Inhibitor for Copper in 3.5% NaCl. *J. Mol. Liq.* **2019**, *289*, 111113.

(58) Smith, R. M.; Sayen, S.; Nuns, N.; Berrier, E.; Guillon, E. Combining Sorption Experiments and Time of Flight Secondary Ion Mass Spectrometry (ToF-SIMS) to Study the Adsorption of Propranolol onto Environmental Solid Matrices - Influence of Copper(II). *Sci. Total Environ.* **2018**, *639*, 841-851.

(59) Martinez-Sanz, M.; Pettolino, F.; Flanagan, B.; Gidley, M. J.; Gilbert, E. P. Structure of Cellulose Microfibrils in Mature Cotton Fibres. *Carbohydr. Polym.* **2017**, *175*, 450-463.

(60) Palza, H. Antimicrobial Polymers with Metal Nanoparticles. *Int. J. Mol. Sci.* **2015**, *16*, 2099-2116.

(61) Rezaie, A. B.; Montazer, M.; Rad, M. M. Environmentally Friendly Low Cost Approach for Nano Copper Oxide Functionalization of Cotton Designed for Antibacterial and Photocatalytic Applications. *J. Cleaner Prod.* **2018**, *204*, 425-436.

(62) Zhu, N.; Zhou, S.; Gong, J.; Wang, X.; Zhang, C.; Li, W.; Sheng, D.; Liu, X.; Xia, L.; Xu, W. In Situ Synthesis of Cuprous Oxide on Cotton Fiber for Developing Functional Textile with Broad-Spectrum Antibacterial Activity. *Ind. Crops Prod.* **2022**, *187*, 115442.

(63) Roman, L. E.; Villalva, C.; Uribe, C.; Paraguay-Delgado, F.; Sousa, J.; Vigo, J.; Vera, C. M.; Gomez, M. M.; Solis, J. L. Textiles Functionalized with Copper Oxides: A Sustainable Option for Prevention of COVID-19. *Polymers.* **2022**, *14*, 3066.

(64) Mathanmohun, M.; Sagadevan, S.; Rahman, M. Z.; Lett, J. A.; Fatimah, I.; Moharana, S.; Garg, S.; Al-Anber, M. A. Unveiling Sustainable, Greener Synthesis Strategies and Multifaceted Applications of Copper Oxide Nanoparticles. *J. Mol. Struct.* **2024**, *1305*, 137788.